Malaysian Journal of Analytical Sciences (MJAS)



Published by Malaysian Analytical Sciences Society

RAPID SYNTHESIS AND CHARACTERIZATION OF VERTICALLY-ALIGNED ZINC OXIDE NANOWIRES BY HYBRID MICROWAVE-ASSISTED SONOCHEMICAL TECHNIQUE

(Sintesis Pantas dan Pencirian Nanowayar Zink Oksida Menegak Sejajar oleh Teknik Hibrid Sonokimia Dibantu Ketuhar Gelombang Mikro)

Maryam Mohammad^{1,2,3}, Mohd Firdaus Malek^{2,3,*}, Muhammad Faizal Abd Halim^{2,3}, Irmaizatussyehdany Buniyamin^{2,3}, Nur Fairuz Rostan^{2,3}, Nurul Zulaikha Mohammad Zamri^{2,3}, Nurfatini Atiqrah Khairul Azhar^{2,3}, Zahidah Othman^{2,3}, Rabiatuladawiyah Md Akhir^{2,3}, Kevin Alvin Eswar^{3,5}, Mohamad Hafiz Mamat⁴, Zuraida Khusaimi^{2,3}, and Mohamad Rusop Mahmood^{2,3,4}

¹Department of Physics, Faculty of Applied Sciences, Universiti Teknologi MARA Perak Branch, Tapah Campus, 35400 Tapah Road, Perak, Malaysia

²School of Physics and Materials Studies, Faculty of Applied Sciences

³NANO-SciTech Lab (NST), Centre for Functional Materials and Nanotechnology (FMN), Institute of Science (IOS)

⁴NANO-ElecTronic Centre (NET), Faculty of Electrical Engineering, Universiti Teknologi MARA (UiTM), 40450 Shah Alam,

Selangor, Malaysia

⁵Faculty of Applied Sciences, Universiti Teknologi MARA Sabah Branch, Tawau Campus, 91032 Tawau, Sabah, Malaysia

*Corresponding author: mfmalek07@uitm.edu.my; mfmalek07@gmail.com

Received: 20 September 2023; Accepted: 30 June 2024; Published: 27 October 2024

Abstract

Zinc oxide nanowires (ZnO NWs) have attracted a lot of attention due to their special characteristics and wide range of uses in nanoelectronics, photonics, sensing, and energy harvesting. Conventional synthesis methods for ZnO NWs often face challenges, such as slow reaction times, limited control over NW shape, and poor scalability. Therefore, it is imperative to develop an advanced synthesis technique that can rapidly produce ZnO NWs while allowing precise control over their structural and functional characteristics. In this study, ZnO NWs were successfully synthesized using a hybrid microwave-assisted sonochemical technique (HMAST) using zinc acetate dihydrate as the starting material. The optimized parameters were set at a solution concentration of 12.5 mM and microwave deposition power of 600 W. The deposition time was varied from 15 to 90 min, and the effect of different deposition times on the morphological, structural, and optical properties of the ZnO NWs was also studied. The samples were characterized by field emission scanning electron microscopy (FESEM), X-ray diffraction (XRD), and ultraviolet-visible (UV-Vis) spectroscopy. The results revealed the production of aligned, uniformly distributed hexagonal wurtzite structure of ZnO NWs with an average diameter size of approximately 31.9 nm. The XRD spectra indicated highly crystalline ZnO NWs, showing the sharpest and narrowest intensity of (002) peaks. The UV-Vis spectra showed high transmittance spectra and a sharp absorption edge, suggesting the smaller particle size of ZnO and strong absorbance in the UV region. From the findings, it can be confirmed that the properties of ZnO NWs produced are controllable by adjusting the deposition time in the HMAST, leading to the formation of high-quality ZnO NWs.

Keywords: zinc oxide, nanowires, nanostructures, microwave-assisted, sonochemical

Abstrak

Nanowayar zink oksida (ZnO NWs) telah menarik banyak perhatian kerana ciri-ciri istimewa dan pelbagai kegunaan mereka dalam bidang nanoelektronik, fotonik, penderiaan, dan pengumpulan tenaga. Kaedah sintesis konvensional untuk ZnO NWs sering menghadapi masalah seperti waktu tindak balas yang lambat, kawalan yang terhad terhadap pembentukan NWs, dan kebolehskalaan yang kurang baik. Oleh itu, teknik sintesis yang canggih yang boleh menghasilkan ZnO NWs dalam masa yang lebih singkat dan mempunyai kawalan yang baik terhadap ciri-ciri struktur dan fungsi mereka adalah penting untuk dicipta. Dalam kajian ini, ZnO NWs telah berjaya disintesis melalui teknik hibrid sonokimia berbantu gelombang mikro (HMAST) dengan menggunakan zink asetat dihidrat sebagai bahan pemula. Parameter yang dioptimumkan ditetapkan pada kepekatan larutan 12.5 mM dan kuasa pengendapan gelombang mikro 600 W. Masa pengendapan diubah dari 15 hingga 90 min, dan kesan perubahan masa pengendapan ke atas sifat morfologi, struktur, dan optik ZnO NWs juga telah dikaji. Sampel-sampel dicirikan oleh mikroskopi elektron pengimbasan pancaran medan (FESEM), pembelauan sinar-X (XRD), dan spektroskopi ultraungu-tampak (UV-Vis). Hasil kajian menunjukkan struktur heksagon wurtzit ZnO NWs yang sejajar dan teragih dengan baik telah dihasilkan, dengan saiz diameter purata lebih kurang 31.9 nm. Spektrum XRD menunjukkan bahawa ZnO NWs yang dihasilkan mempunyai kehabluran yang sangat tinggi dan menunjukkan puncak (002) yang paling tajam dan lebih halus. Spektrum UV-Vis menunjukkan spektrum kepancaran yang tinggi berserta kesan penyerapan yang jelas, menunjukkan saiz zarah ZnO yang lebih kecil serta penyerapan yang tinggi dalam julat UV. Berdasarkan penemuan ini, sifat-sifat ZnO NWs yang dihasilkan dapat disahkan boleh dikawal dengan mengubah masa pengendapan bagi kaedah HMAST, seterusnya membawa kepada pembentukan ZnO NWs yang lebih berkualiti.

Kata kunci: zink oksida, nanowayar, nanostruktur, bantuan gelombang mikro, sonokimia

Introduction

Zinc oxide (ZnO) is one of the many nanostructured materials frequently used in the research and development of oxide-based multifunctional materials and one-dimensional nanostructures (1-D NSs) due to its excellent and unique properties, and one of its notable characteristics is its ability to enhance the performance of electrical devices such as sensors, converters, energy generators, and many more [1, 2]. Furthermore, within the category of group II-VI semiconductors, ZnO is classified as having a covalent link with an ionic atom. It is attractive for potential applications in electronics, optoelectronics, and laser technologies due to its wide energy band (3.37 eV), high bond energy (60 meV), and outstanding thermal and mechanical stability at ambient temperature [3-6]. Zinc oxide nanowires (ZnO NWs) with their large surface-to-volume ratios and quasi-1-D structures exhibiting quantum confinement effects, stand out among other NSs. They can be viewed as 1-D channels that conduct electrons, holes, and photons through absorption, emission, and transport. This results in strong confinement effects on the carriers and photons, leading to a variety of new optical and electrical properties suitable for device applications such as short-wavelength light-emitting diodes and nanometer lasers [7]. It has also been discovered that compared to nanoparticles (NPs) deposited on a flat

surface, 1-D NSs, such as NWs grown on a substrate, offer higher surface-to-volume ratios, thereby enhancing photocatalytic activity through improved adsorption of target organic molecules onto the catalyst surface [8, 9]. Furthermore, as compared to other semiconductors utilized in nanotechnology, ZnO NWs, with their simple crystal growth process, offer lower production costs due to the wide range of substrate materials and geometries [10, 11]. Various growth methods, including chemical and physical techniques, have been applied for the production of ZnO NWs with preferable vertically-aligned orientation, such as thermal evaporation [12-14], chemical vapor deposition (CVD) and cyclic feeding CVD [15, 16], sol-gel deposition [17, 18], electrochemical deposition [19, 20], hydrothermal and solvothermal growth [21-26], and surfactant and capping agent-assisted growth [27, 28].

However, the drawback of these methods is that they must be used under extreme conditions (e.g., high temperatures and pressures), in addition to expensive materials and complicated procedures [29]. For instance, the widely used conventional approach for producing ZnO NWs via a solution-based method tends to overlook the importance of the solution preparation process. Instead, it predominantly focuses on the effect of stabilizers rather than ensuring proper dispersion of

reactants, leading to a non-homogeneous reaction during the precursor and solvent mixing process. This discrepancy contributes to the formation of larger particle sizes and reduces the surface area of the NSs. Consequently, the presence of defects, such as grain boundaries, hinders electron transport and promotes high recombination of electrons [30]. Furthermore, prevalent growth methods for ZnO NWs, such as thermal evaporation, CVD, sol-gel deposition, electrochemical deposition, hydrothermal solvothermal growth, as well as surfactant and capping agent-assisted growth, which are known for their synthesis success rates, suffer from certain drawbacks, such as low productivity or significant impurities introduced by the catalysts or precursors, requiring a prolonged deposition period that complicates their application in their targeted nanodevices [31].

Microwave-assisted process has been recommended by many researchers due to its numerous benefits, including low cost, convenience of use, minimal energy usage, and scalability [32-33]. This is mostly due to the mechanism of microwaves, which can address limitations, as well as improve the synthesis process and the material quality of ZnO NWs. Microwaves fall within a region of the electromagnetic spectrum that has a wavelength (λ) between 1 mm and 1 m, or a frequency range between 300 MHz ($\lambda = 1$ m) and 300 GHz ($\lambda = 1$ mm) [34, 35]. Its numerous benefits, including scalability, low energy consumption, quick growth, low cost, and simplicity of handling, make it a highly acclaimed method for addressing issues [36-39]. Moreover, compared to conventional ZnO NWs produced by traditional methods, the microwaveassisted process offers more control over the shape and dimensional dispersion of ZnO NWs, ensuring greater consistency in experimental results [40]. Microwave irradiation is essential for chemical reactions in aqueous media [41], reducing time [42] and costs, decreasing particle size with a narrow size distribution, increasing product yield rates, and producing high-purity yields [43-46].

Our study focuses on overcoming the common problem of prolonged synthesis time and non-homogeneous mixing process resulting in large particle size, lower surface area, reduced electron transit, and excessive recombination [47]. In contrast to conventional microwave methods, the hybrid microwave-assisted sonochemical technique (HMAST) integrates a highly and commonly used solution-based effective (sonochemical) technique during the mixing process to significantly improve the homogeneity of the solution and the interaction between the precursor and the stabilizing agent, thereby providing better overall control of the features of the NWs. Additionally, this method is further assisted by microwave irradiation to expedite the production process. Therefore, the investigation on the effect of deposition time on the ZnO NWs produced by the HMAST aims to demonstrate a faster, more controlled, and scalable production of NWs. This approach could also contribute to advancements in various applications involving ZnO NWs, given the controllable nature of the HMAST in modifying the properties of ZnO NWs to meet the specific requirements of the device or application.

Materials and Methods

The research approach is divided into three parts, which are outlined as follows. The initial step involves preparing and cleaning the glass substrates. Subsequently, the ZnO NPs thin film was prepared using an ultrasonic-assisted sol-gel (sonochemical) spin coating process, resulting in the ZnO NPs arrays. The next step involves a microwave heating deposition process to produce ZnO NWs.

Preparation of ZnO NPs seeded layer thin films

Zinc oxide-based NPs were prepared as a seed layer of thin films on a glass substrate, which was deposited by an optimized ultrasonic-assisted sol-gel (sonochemical) spin-coating technique [47, 48]. The sonicated sol-gel ZnO was prepared by dissolving 0.4 M zinc acetate dihydrate (Zn(CH₃COO)₂·2H₂O; Merck), which acts as the precursor in the solvent of 2-methoxy ethanol (C₃H₈O₂; Merck) at room temperature. Then, 1% aluminum nitrate nonahydrate (Al(NO₃)₃·9H₂O; Analar) and 0.4% monoethanolamine (MEA, C₂H₇NO; R&M) were added into the solution as a dopant and stabilizer, respectively. The molar ratio of MEA to zinc acetate dihydrate was maintained at 1:1, and the resulting solution was stirred at 80 °C for 40 min to yield

a clear and homogeneous solution. Afterward, the solution was sonicated at 50 °C for 30 min using an ultrasonic water bath (Hwasin Technology Powersonic 405, 40 kHz) and cooled to room temperature. The solution was used to coat the glass substrate using the spin coating technique, where ten drops of the solution were deposited onto the substrate at a speed of 3,000

rpm for 30 s. Lastly, the samples were preheated in an ambient atmosphere at 300 °C for 10 min to remove the solvent, and the deposition processes were repeated for the second to the fifth layer of the film to achieve the required film thickness. All samples were annealed in a furnace at a temperature of 500 °C for 1 h. The procedures described above are depicted in Figure 1.

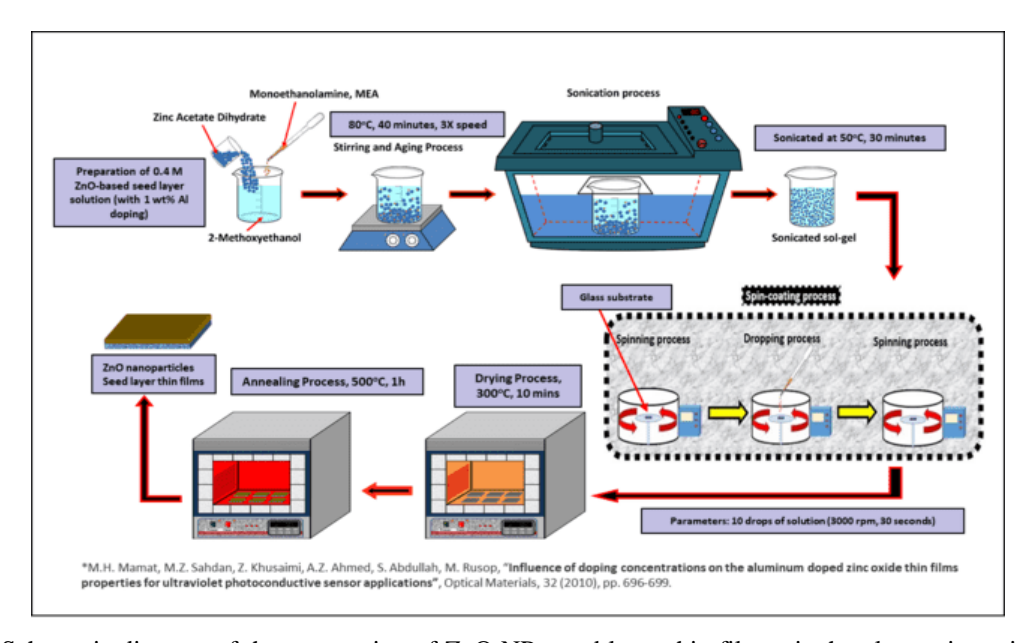


Figure 1. Schematic diagram of the preparation of ZnO NPs seed layer thin films via the ultrasonic-assisted sol-gel (sonochemical) spin coating technique

Deposition of ZnO NWs via the HMAST

ZnO NWs were grown via the HMAST. An optimized solution with a concentration of 12.5 mM was prepared dihydrate using zinc acetate and 0.01 hexamethylenetetramine (HMTA, C₆H₁₂N₄; Merck) as a precursor and stabilizer, respectively [49]. The reagents were dissolved and reacted in a beaker containing 1,000 mL of distilled water as a solvent and stirred at 80 °C for 30 min to obtain a clear and homogeneous solution. Subsequently, the solution was sonicated at 50 °C for 30 min using the ultrasonic water bath at 40 kHz. The solution was then aged at room temperature for 1 h before being transferred into a 250 mL Schott bottle, where the optimized seed layer-coated glass substrates were placed at the bottom of the container. Afterward, the container was inserted into a 2.45 GHz microwave

(SHARP 25 L Microwave Oven R352ZS) set at a microwave power of 600 W and a frequency of 2.45 GHz for durations of 15, 30, 45, 60, 75, and 90 min each. Following this, the samples were annealed at a temperature of 500 °C for 1 h. These procedures are illustrated in Figure 2.

Characterization method

The structural and morphological properties of ZnO NWs were characterized using X-ray diffraction (XRD, PANalytical X'Pert PRO) with Cu-Kα radiation of a wavelength of 1.54 Å and field emission scanning electron microscopy (FESEM, JEOL JSM-7600F). The optical properties were characterized by ultravioletvisible (UV-Vis) spectroscopy (Cary 5000).

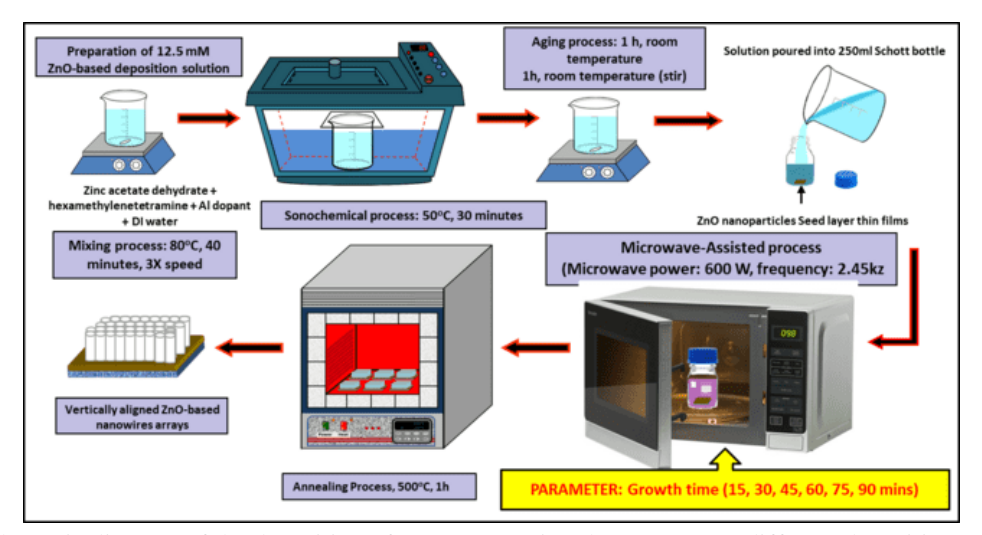


Figure 2. Schematic diagram of the deposition of ZnO NWs using the HMAST at different deposition temperatures

Results and Discussion

Morphological and structural study

Figures 3 (a)–(f) show a clear top view of FESEM images of the ZnO NWs synthesized using the HMAST at different deposition times. It was found that the ZnO NWs were vertically oriented and densely packed on all the substrates. As the deposition time increased, some of the shapes of the ZnO NWs were not perfectly hexagonal and began tilting toward one another. This phenomenon is attributed to the interfacial surface energy and capillarity between the adjoining ZnO NWs, which allows them to tilt and merge into one another [50]. It can also be seen that the ZnO NWs deposited at 60-90 min reaction time were longer in length but similar in size. The measurements were averaged from individual NWs based on each sample's area distribution of NWs, determined using ImageJ software. The average diameter size distribution of the NWs was determined to be approximately 30 nm, as tabulated in Table 1, and this was confirmed from their respective particle size distribution histogram, as shown in Figure 4. The structure of the ZnO NWs was also affected by variations in the deposition time, where the crystallite size increased from 33 nm at 15 min deposition time to 52.21 nm at the longest deposition time of 90 min. The shorter deposition time enables rapid nucleation, whereby small crystallite size leads to an increased aspect ratio and the availability of active sites [51-53].

ZnO NWs exhibit anisotropic growth due to variations in the growth kinetics along different crystallographic directions. The slight changes in the orientation of NWs might also be due to the crystal growth anisotropy. Owing to the thermodynamic and kinetic factors associated with these aspects, during the initial stages of growth, NWs may exhibit a preference for nucleation and grow along certain crystallographic facets with lower energy. However, as the NWs lengthen with longer deposition times, the rates of development of certain facets may change, resulting in modifications to the overall orientation of the NWs, as confirmed in the XRD spectra analysis. Longer deposition times can also lead to a diffusion-limited growth regime, as discussed by Rana et al., where the availability of precursor molecules becomes a limiting factor. In our experiment, the amount of deposition solution used is not continuous and can only last for a certain period of time at the optimized microwave power of 600 W. Additionally, the study conducted by Abu ul Hassan et al. found that microwave heating provides homogeneous heat transfer to the solution mixture for chemical reactions, thereby accelerating the synthesis process, as evidenced by all the samples of ZnO NWs produced by the HMAST, where the NWs were synthesized at a rapid deposition time of as little as 15 min [54].

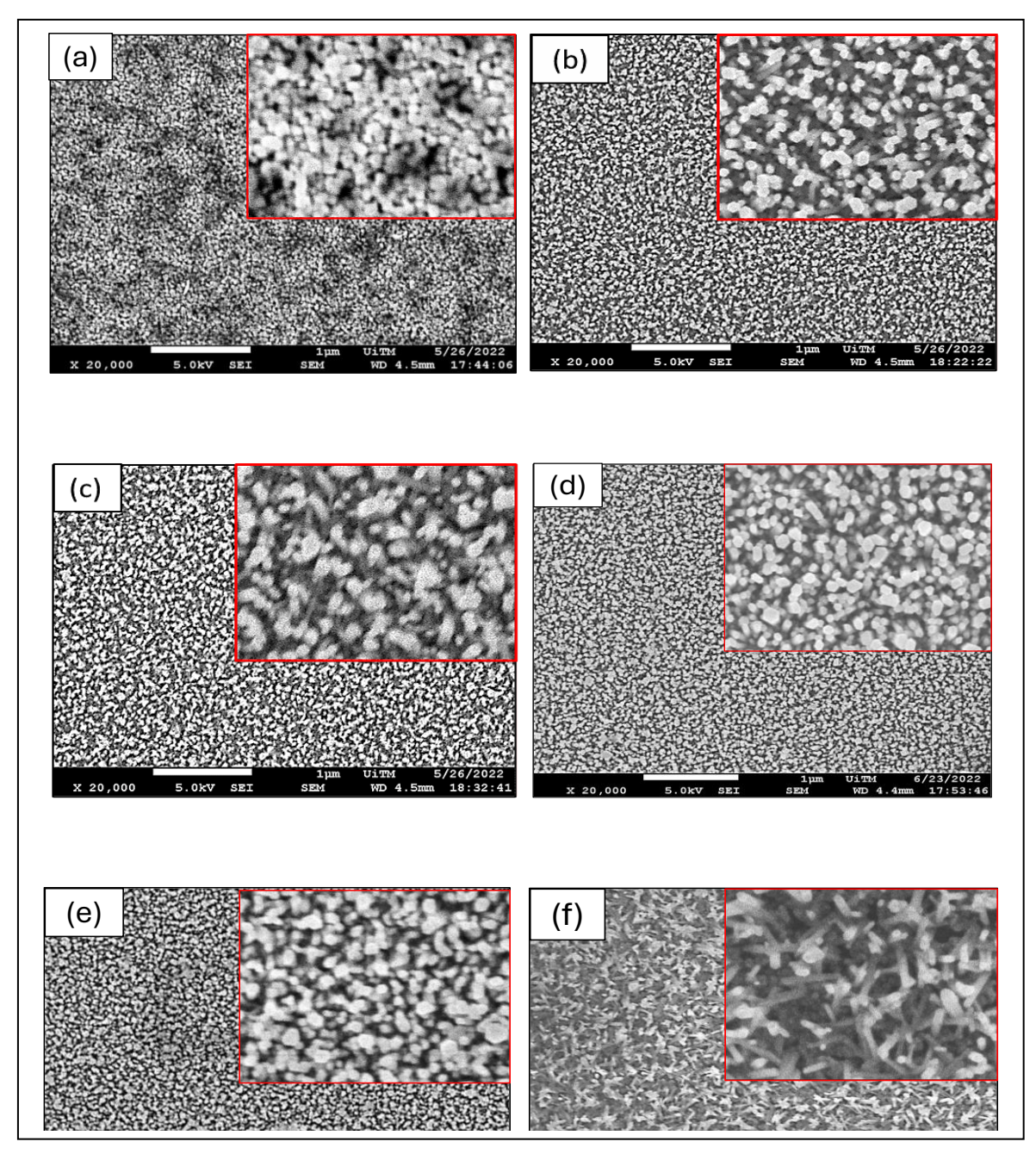


Figure 3. FESEM images at $20,000\times$ and $100,000\times$ magnification (upper insets) of ZnO NWs synthesized using the HMAST at different deposition times of (a) 15 min, (b) 30 min, (c) 45 min, (d) 60 min, (e) 75 min, and (f) 90 min

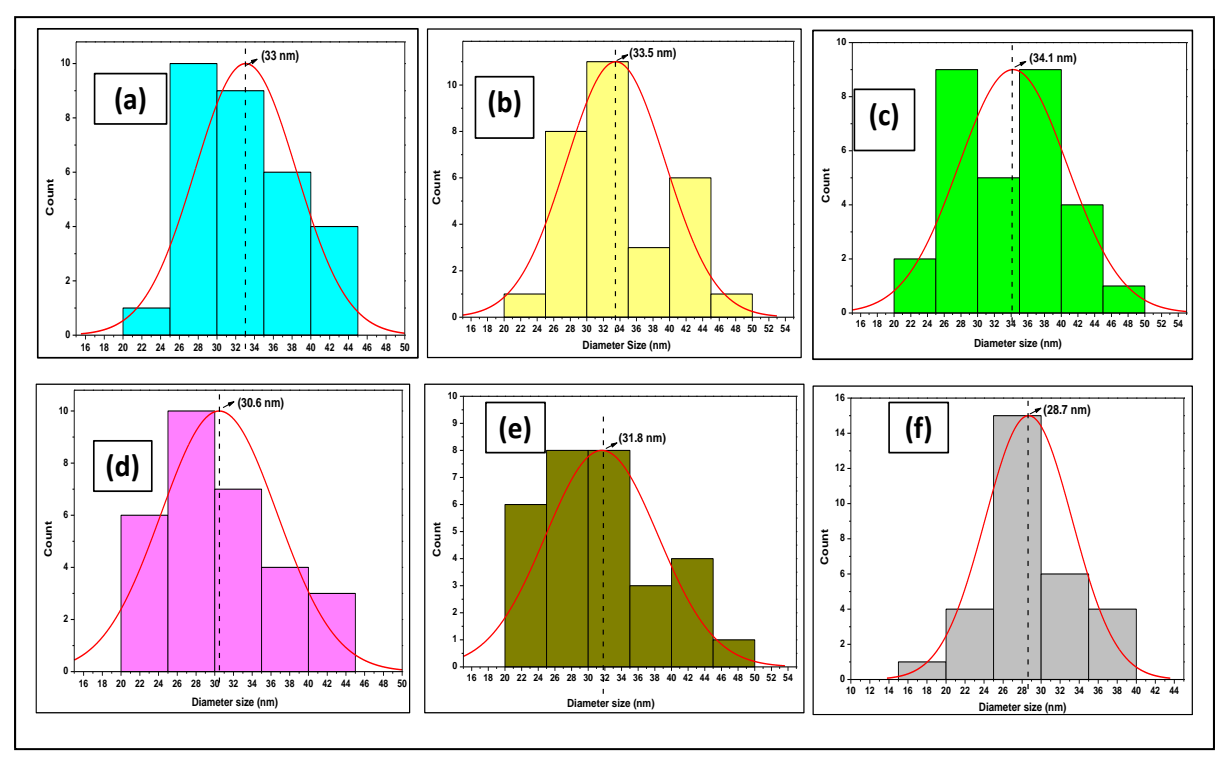


Figure 4. Particle size distribution diagrams of ZnO NWs synthesized using the HMAST at different deposition times of (a) 15 min, (b) 30 min, (c) 45 min, (d) 60 min, (e) 75 min, and (f) 90 min

The XRD spectra of the ZnO NWs fabricated using the HMAST are shown in Figure 5 at various deposition times. The Joint Committee on Powder Diffraction Standards (JCPDS) database of ZnO hexagonal structure was used to index the numerous XRD peaks (File No. 36-1451). The ZnO NWs prepared from each sample exhibited a high degree of crystallinity with a hexagonal wurtzite structure and a preferred c-axis orientation. They also have six distinct diffraction peaks that were detected between 20° and 70°. The maximum intensity of these peaks was indexed at planes (100), (101), and (002), while the lowest intensity was observed at planes (102), (110), and (112). The ZnO NWs also exhibited a clear and similar trend of increasing crystallite size with longer deposition times, as presented in Table 1. The observations of all the grown NWs indicated that the particles preferentially grew in one direction, resulting in structures that are almost 1-D or rod-like, with the most prominent (002) orientation peak ranging from 33.86° to 33.90°. On the contrary, the lower intensities of the other peaks could be attributed to a few misaligned ZnO NWs growing on the glass substrate. In general, the synthesized NWs only exhibit distinct crystalline structures without any other phases, such as amorphous structures, being present. This outcome is consistent with those mentioned in previous studies [55, 56].

The average crystallite size D (nm) of the ZnO NWs was calculated using Scherrer's formula as follows.

$$D = \frac{0.9\lambda}{\beta \cos \theta}$$

Where λ is the X-ray wavelength of Cu-K α radiation source (λ = 1.5418A°), β (in radians) is the full-width at half-maximum (FWHM) intensity of the diffraction peak located at 2 θ , and θ is the Bragg's angle. The calculated results are shown and summarized in Table 1. It was discovered that the average crystallite size increased from 34.67 to 52.21 nm with an increase in deposition time from 15 to 90 min, consistent with the particle size observed in FESEM. Although ZnO NWs can be grown in powder form, our method utilizes

substrates, specifically low-cost soda lime silica glass because vertically-oriented growth on a substrate offers significant benefits, particularly for photocatalytic applications. The formation of NWs is aided by the anisotropy of the ZnO crystal structure. The basal plane

(001) consists of partially positive Zn lattice points at one end and partially negative oxygen lattice points at the other end and follows the following pattern: $\nu_{(0001)} > \nu_{(01\overline{11})} > \nu_{(01\overline{10})} > \nu_{(01\overline{11})} > \nu_{(000\overline{1})}$ [57].

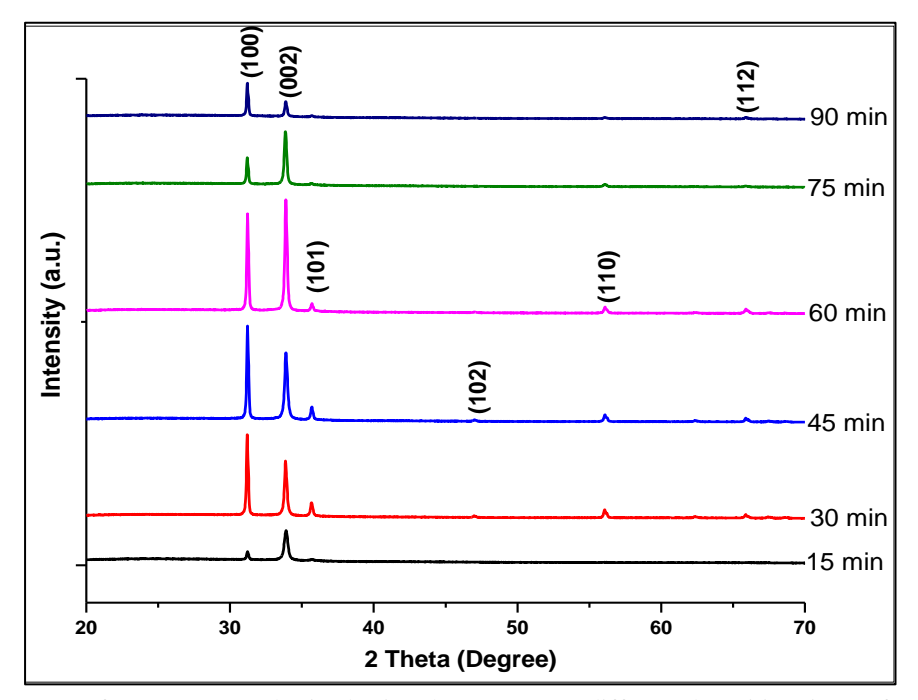


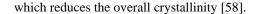
Figure 5. XRD spectra of ZnO NWs synthesized using the HMAST at different deposition times of (a) 15 min, (b) 30 min, (c) 45 min, (d) 60 min, (e) 75 min, and (f) 90 min

Table 1. Structural parameters of ZnO NWs synthesized using the HMAST at different deposition times of (a) 15 min, (b) 30 min, (c) 45 min, (d) 60 min, (e) 75 min, and (f) 90 min

Sample	Growth Time	Peak Position	FWHM	Crystallite	Diameter Size
	(min)	(20)	(°)	Size (nm)	(nm)
(a)	15	33.90	0.250	34.67	33.0
(b)	30	33.87	0.189	45.86	33.5
(c)	45	33.90	0.186	46.10	34.1
(d)	60	33.89	0.183	50.68	30.6
(e)	75	33.86	0.169	51.28	31.8
(f)	90	33.89	0.166	52.21	28.7

Likewise, the intensity of the XRD peak at the (002) plane increased below 60 min deposition time, which can be attributed to the nearly perfect alignment of the NWs. However, the intensity of the XRD peaks for NWs deposited at 60 min deposition time onwards decreased, which aligns with the SEM analysis discussed earlier, where the orientation of the NWs had changed, leading

to an increase in the intensity of other peaks, particularly the (100) peak. This might also be due to the Ostwald ripening phenomenon, where the smaller crystallites dissolve and redeposit on larger ones, leading to the growth of larger crystals at the expense of smaller ones. During longer deposition times, this process can occur and lead to the merging of smaller crystalline domains,



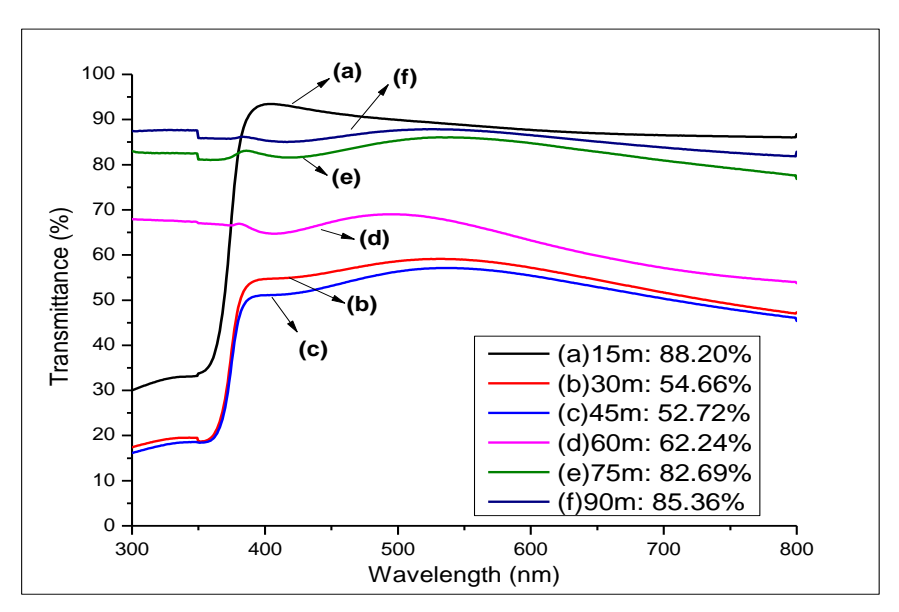


Figure 6. Transmittance spectra of ZnO NWs synthesized using the HMAST at different deposition times of (a) 15 min, (b) 30 min, (c) 45 min, (d) 60 min, (e) 75 min, and (f) 90 min

The optical properties of the synthesized ZnO NWs evaluated using UV-Vis spectrometer measurements conducted between 200 and 800 nm at room temperature. There is a migration of the absorption band edge toward the visible region and a dependence on the precursor in the optical absorption spectra of all synthesized ZnO samples in the visible and UV ranges. Figure 6 displays the transmittance spectra of the ZnO NWs fabricated using the HMAST at different deposition solution concentrations. The transmittance spectra in the entire visible range displayed an exciton peak in the 350-380 nm range and reduced absorbance beyond 380 nm. Strong absorbance in the UV spectrum indicates high crystallinity, whereas sharp absorption edges suggest smaller ZnO particle sizes [59]. The highest transmittance was recorded for the sample synthesized at 15 min deposition time, as shown in Figure 6 (a), with an average transmittance of 88.20% between 400 and 800 nm in the visible region. In contrast, the lowest transmittance was obtained for the NWs deposited within 45 min (Figure 6 (c)), with an average transmittance of 52.72% over the same wavelength. It can also be seen from Figures 6 (a)–(c) that the transmittance decreased as the deposition time increased from 15 to 45 min and started to increase from

60 min onward (Figures 6 (d)–(f)). The significant changes in the transmittance spectra might be due to the change in the structural properties as discussed previously. The changes in the transmission spectrum could also be caused by interferences in thin films resulting from reflection at the air-ZnO and ZnO-glass interfaces [60]. Overall, all the samples show varying levels of transparency and can be applicable in various applications. Most importantly, it has the highest transmittance within the shortest deposition time of 15 min. This suggests that the ZnO NWs produced through rapid deposition by the HMAST can be used in electrical devices, such as the window layer in solar cells, to efficiently capture photons.

Conclusions

In conclusion, highly crystalline ZnO NWs with a hexagonal wurtzite structure and a preferred c-axis orientation were successfully synthesized using a novel HMAST at different short deposition times of 15–60 min with a significant improvement in their properties. It was found that the peak intensities of the ZnO NWs increased as the deposition time increased up to 60 min, indicating the high purity of the produced ZnO NWs. The trend in the growth of the aligned ZnO NWs arrays

is supported by the FESEM images of the samples, which indicate a very small average diameter of approximately 30 nm of all NWs. The XRD analysis provided structural insights, revealing significant phase identification according to JCPDS (File No 36-1451), with strong and narrow peak intensities observed for the (100), (002), and (101) peaks, and an increase in crystallite size with time. The optical analysis of the samples revealed that the ZnO NWs obtained by this method exhibited the highest transmittance of approximately 88.20% with the shortest deposition time. As evidenced, the HMAST continues to be an active area of investigation with a potential impact on the rapid growth of ZnO NWs; hence, future work may be conducted based on recent findings. Through continued exploration and validation, this technique holds the promise to drive advancements in various technological applications and contribute to the growing body of knowledge in nanomaterial synthesis.

Acknowledgment

This work was supported in part by grant No. 600-RMC/GPM CoE 5/3 (106/2022). The authors would like to thank the Research Management Centre (RMC), Universiti Teknologi MARA (UiTM), Malaysia, for their support. The authors would also like to thank Mr. Salifairus Mohammad Jafar (UiTM Senior Science Officer), Ts. Irmaizatussyehdany Buniyamin (UiTM Senior Research Officer), and Mr. Mohd Azlan Jaafar (UiTM Assistant Engineer) for their kind support of this research.

References

- Theerthagiri, J., Salla, S., Senthil, R. A., Nithyadharseni, P., Madankumar, A., Arunachalam, P., ... and Kim, H. S. (2019). A review on ZnO nanostructured materials: energy, environmental and biological applications. *Nanotechnology*, 30(39): 392001.
- Tajik, S., Beitollahi, H., Shahsavari, S., and Nejad, F. G. (2022). Simultaneous and selective electrochemical sensing of methotrexate and folic acid in biological fluids and pharmaceutical samples using Fe₃O₄/ppy/Pd nanocomposite modified screen printed graphite electrode. *Chemosphere*, 291: 132736.

- Chaari, M., and Matoussi, A. (2012). Electrical conduction and dielectric studies of ZnO pellets. *Physica B: Condensed Matter*, 407(17): 3441-3447.
- Shohany, B. G., and Zak, A. K. (2020). Doped ZnO nanostructures with selected elements-Structural, morphology and optical properties: A review. Ceramics International, 46(5): 5507-5520.
- Bhati, V. S., Hojamberdiev, M., and Kumar, M. (2020). Enhanced sensing performance of ZnO nanostructures-based gas sensors: A review. *Energy Reports*, 6: 46-62.
- Sheikh, M., Pazirofteh, M., Dehghani, M., Asghari, M., Rezakazemi, M., Valderrama, C., and Cortina, J. L. (2020). Application of ZnO nanostructures in ceramic and polymeric membranes for water and wastewater technologies: A review. *Chemical Engineering Journal*, 391: 123475.
- 7. Cui, J. (2012). Zinc oxide nanowires. *Materials Characterization*, 64: 43-52.
- 8. Zhou, Q., Wen, J. Z., Zhao, P., and Anderson, W. A. (2017). Synthesis of vertically-aligned zinc oxide nanowires and their application as a photocatalyst. *Nanomaterials*, 7(1): 9.
- Galdámez-Martinez, A., Santana, G., Güell, F., Martínez-Alanis, P. R., and Dutt, A. (2020). Photoluminescence of ZnO nanowires: A review. *Nanomaterials*, 10(5): 857.
- Cristina V. Manzano, Laetitia, P. and Albert, S. (2022). Recent progress in the electrochemical deposition of ZnO nanowires: synthesis approaches and applications, *Critical Reviews in Solid State and Materials Sciences*, 47(5): 772-805.
- 11. Zhang, Y., Ram, M. K., Stefanakos, E. K. and Goswami, D. Y. (2012). Synthesis, characterization, and applications of ZnO nanowires. *Journal of Nanomaterials*, 2012(1): 624520.
- Van Khai, T., Thanh, V. M., and Dai Lam, T. (2018)
 Structural, optical and gas sensing properties of
 vertically well-aligned ZnO nanowires grown on
 graphene/Si substrate by thermal evaporation
 method. *Materials Characterization*, 141: 296-317.
- 13. Alia Azmi, F. F., Sahraoui, B., and Muzakir, S. K. (2019). Study of ZnO nanospheres fabricated via thermal evaporation for solar cell application. *Makara Journal of Technology*, 23(1): 2.

- 14. Ahmoum, H., Li, G., Belakry, S., Boughrara, M., Su'ait, M. S., Kerouad, M., and Wang, Q. (2021). Structural, morphological and transport properties of Ni doped ZnO thin films deposited by thermal co-evaporation method. *Materials Science in Semiconductor Processing*, 123: 105530.
- Narin, P., Kutlu-Narin, E., Kayral, S., Tulek, R., Gokden, S., Teke, A., and Lisesivdin, S. B. (2022). Morphological and optical characterizations of different ZnO nanostructures grown by mist-CVD. *Journal of Luminescence*, 251: 119158.
- Bai, M., Chen, M., Li, X., and Wang, Q. (2022).
 One-step CVD growth of ZnO nanorod/SnO₂ film heterojunction for NO₂ gas sensor. Sensors and Actuators B: Chemical, 373: 132738.
- Amakali, T., Daniel, L. S., Uahengo, V., Dzade, N. Y., and De Leeuw, N. H. (2020). Structural and optical properties of ZnO thin films prepared by molecular precursor and sol–gel methods. *Crystals*, 10(2): 132.
- 18. Ebrahimifard, R., Abdizadeh, H., and Golobostanfard, M. R. (2020). Controlling the extremely preferred orientation texturing of sol—gel derived ZnO thin films with sol and heat treatment parameters. *Journal of Sol-Gel Science and Technology*, 93: 28-35.
- Qiao, F., Liang, Q., Yang, J., Chen, Z., and Xu, Q. (2019). A facile approach of fabricating various ZnO microstructures via electrochemical deposition. *Journal of Electronic Materials*, 48: 2338-2342.
- Pruna, A., Wu, Z., Zapien, J. A., Li, Y. Y., and Ruotolo, A. (2018). Enhanced photocatalytic performance of ZnO nanostructures by electrochemical hybridization with graphene oxide. *Applied Surface Science*, 441: 936-944.
- Gerbreders, V., Krasovska, M., Sledevskis, E., Gerbreders, A., Mihailova, I., Tamanis, E., and Ogurcovs, A. (2020). Hydrothermal synthesis of ZnO nanostructures with controllable morphology change. *CrystEngComm*, 22(8): 1346-1358.
- Katiyar, A., Kumar, N., Shukla, R. K., and Srivastava, A. (2020). Substrate free ultrasonicassisted hydrothermal growth of ZnO nanoflowers at low temperature. SN Applied Sciences, 2: 1-7.
- 23. Faisal, A. D., Ismail, R. A., Khalef, W. K., and

- Salim, E. T. (2020). Synthesis of ZnO nanorods on a silicon substrate via hydrothermal route for optoelectronic applications. *Optical and Quantum Electronics*, 52: 1-12.
- 24. Zare, M., Namratha, K., Byrappa, K., Surendra, D.M., Yallappa, S., and Hungund, B. (2018). Surfactant assisted solvothermal synthesis of ZnO nanoparticles and study of their antimicrobial and antioxidant properties *Journal of Materials Science & Technology*, 34(6): 1035-1043.
- Mao, Y., Li, Y., Zou, Y., Shen, X., Zhu, L., and Liao, G. (2019). Solvothermal synthesis and photocatalytic properties of ZnO micro/nanostructures. *Ceramics International*, 45(2): 1724-1729.
- Zhang, X., Chen, J., Wen, M., Pan, H., and Shen, S. (2021). Solvothermal preparation of spindle hierarchical ZnO and its photocatalytic and gas sensing properties. *Physica B: Condensed Matter*, 602: 412545.
- Zhao, S., Shen, Y., Yan, X., Zhou, P., Yin, Y., Lu, R., ... and Wei, D. (2019). Complex-surfactant-assisted hydrothermal synthesis of one-dimensional ZnO nanorods for high-performance ethanol gas sensor. Sensors and Actuators B: Chemical, 286: 501-511.
- Basnet, P., & Chatterjee, S. (2020). Structure-directing property and growth mechanism induced by capping agents in nanostructured ZnO during hydrothermal synthesis—A systematic review. Nano-Structures & Nano-Objects, 22: 100426.
- Ghazali, M. N. I., Izmi, M. A., Mustaffa, S. N. A., Abubakar, S., Husham, M., Sagadevan, S., & Paiman, S. (2021). A comparative approach on One-Dimensional ZnO nanowires for morphological and structural properties. *Journal of Crystal Growth*, 558: 125997.
- Messih, M. A., Ahmed, M. A., Soltan, A., and Anis, S. S. (2019). Synthesis and characterization of novel Ag/ZnO nanoparticles for photocatalytic degradation of methylene blue under UV and solar irradiation. *Journal of Physics and Chemistry of Solids*, 135: 109086.
- Ma, G., Zhu, Y., Cheng, G., and Huang Y. H. (2008). Microwave synthesis and characterization of ZnO with various morphologies. *Material*

- Letters, 62: 10-507.
- 32. Kajbafvala, A., Shayegh, M. R., Mazloumi, M., Zanganeh, S., Lak, A., Mohajeraniand, M. S., Sadrnezhaad S. K. K. (2009). Nanostructure sword-like ZnO wires: rapid synthesis and characterization through a microwave-assisted route. *Journal Alloys Compounds*, 469: 7-293.
- 33. Ghosh, S., and Chakraborty, J. (2016). Rapid synthesis of zinc oxide nanoforest: use of microwave and forced seeding. *Materials Research Express*, 3(12): 125004.
- 34. Hitchcock, R. T. (2004). Radio-frequency and microwave radiation. American Industrial Hygiene Association.
- 35. Vollmer, M. (2004). Physics of the microwave oven. *Physics Education*, 39: 74–80.
- 36. Mohammadi, E., Aliofkhazraei, M., Hasanpoor, M., & Chipara, M. (2018). Hierarchical and complex ZnO nanostructures by microwave-assisted synthesis: morphologies, growth mechanism and classification. *Critical Reviews in Solid State and Materials Sciences*, 43(6): 475-541.
- 37. Mallikarjunaswamy, C., Lakshmi Ranganatha, V., Ramu, R., Udayabhanu, and Nagaraju, G. (2020). Facile microwave-assisted green synthesis of ZnO nanoparticles: application to photodegradation, antibacterial and antioxidant. *Journal of Materials Science: Materials in Electronics*, 31: 1004-1021.
- 38. Kumar, A., Kuang, Y., Liang, Z., and Sun, X. (2020). Microwave chemistry, recent advancements, and eco-friendly microwave-assisted synthesis of nanoarchitectures and their applications: A review. *Materials Today Nano*, 11: 100076.
- 39. Devi, N., Sahoo, S., Kumar, R., and Singh, R. K. (2021). A review of the microwave-assisted synthesis of carbon nanomaterials, metal oxides/hydroxides and their composites for energy storage applications. *Nanoscale*, 13(27): 11679-11711.
- 40. Garino, N., Limongi, T., Dumontel, B., Canta, M., Racca, L., Laurenti, M., ... and Cauda, V. (2019). A microwave-assisted synthesis of zinc oxide nanocrystals finely tuned for biological applications. *Nanomaterials*, 9(2): 212.
- 41. Rao, K. J., Vaidhyanathan B., Ganguli M., and

- Ramakrishnan P. A. (1999). Synthesis of inorganic solids using microwaves, *Chemistry of Materials*, 11(4): 882-895, 1999.
- 42. Cullity, B. D. (1956). Elements of X-ray diffraction. Addison-Wesley Publishing.
- 43. Kingston H. M., Walter P. J., Chalk S. J., Lorentzen E. and Link D. (1997). Chapter 3: Environmental microwave sample preparation fundamentals, methods, and applications. *Microwave Enhanced Chemistry: Fundamentals, Sample Preparation, and Applications*, pp. 223-349.
- 44. Ahmad, M. M., Kotb, H. M., Mushtaq, S., Waheed-Ur-Rehman, M., Maghanga, C. M., and Alam, M. W. (2022). Green synthesis of Mn⁺ Cu bimetallic nanoparticles using Vinca rosea extract and their antioxidant, antibacterial, and catalytic activities. *Crystals*, 12(1): 72.
- 45. Palchik O., Zhu J. and Gedanken A. (2000). Microwave assisted preparation of binary oxide nanoparticles. *Journal of Materials Chemistry*, 10(5): 1251-1254.
- Horikoshi, S., Schiffmann, R. F., Fukushima, J. and Serpone, N. (2018). Materials processing by microwave heating. *Microwave Chemical and Materials Processing, Springer, Singapore*, pp. 321-381.
- 47. Messih, M. A., Ahmed, M. A., Soltan, A., and Anis, S. S. (2019). Synthesis and characterization of novel Ag/ZnO nanoparticles for photocatalytic degradation of methylene blue under UV and solar irradiation. *Journal of Physics and Chemistry of Solids*, 135: 109086.
- 48. Mamat, M. H., Sahdan, M. Z., Khusaimi, Z., Ahmed, A. Z., Abdullah, S., and Rusop, M. (2010) Influence of doping concentrations on the aluminum doped zinc oxide thin films properties for ultraviolet photoconductive sensor applications. *Optical Materials*, 32(6): 696-699.
- Malek, M. F., Mamat, M. H., Musa, M. Z., Soga, T., Rahman, S. A., Alrokayan, S. A., and Rusop, M. (2015). Metamorphosis of strain/stress on optical band gap energy of ZAO thin films via manipulation of thermal annealing process, *Journal of Luminescence*, 160: 165-175.
- 50. Ge, X., Hong, K., Zhang, J., Liu, L., and Xu, M. (2015). A controllable microwave-assisted

- hydrothermal method to synthesize ZnO nanowire arrays as recyclable photocatalyst, *Materials Letters*, 139: 119-121.
- Rana, A. U. H. S., Kang, M., and Kim, H. S. (2016).
 Microwave-assisted facile and ultrafast growth of ZnO nanostructures and proposition of alternative microwave-assisted methods to address growth stoppage. *Scientific Reports*, 6(1): 24870.
- 52. Amakali, T., Daniel, L. S., Uahengo, V., Dzade, N. Y., and De Leeuw, N. H. (2020). Structural and optical properties of ZnO thin films prepared by molecular precursor and sol–gel methods. *Crystals*, 10(2): 132.
- 53. Mohamed, R., Mamat, M. H., Ismail, A. S., Malek, M. F., Zoolfakar, A. S., Khusaimi, Z., ... and Rusop, M. (2017). Hierarchically assembled tin-doped zinc oxide nanorods using low-temperature immersion route for low temperature ethanol sensing. *Journal of Materials Science: Materials in Electronics*, 28: 16292-16305.
- 54. Mohamed, R., Mamat, M. H., Malek, M. F., Ismail, A. S., Rafaie, H. A., and Rusop, M. (2020). Controllable synthesis of Sn: ZnO/SnO₂ nanorods: pH-dependent growth for an ethanol gas sensor. *Journal of Materials Science: Materials in Electronics*, 31: 15394-15406.
- 55. Messih, M. A., Ahmed, M. A., Soltan, A., and Anis, S. S. (2019). Synthesis and characterization of novel Ag/ZnO nanoparticles for photocatalytic degradation of methylene blue under UV and solar

- irradiation. *Journal of Physics and Chemistry of Solids*, 135: 109086.
- Salah, N., Habib, Khan, Z., Memic, A., Azam, A., Salah, N., Memic, Habib, S, (2011). High-energy ball milling technique for ZnO nanoparticles as antibacterial material. *International Journal Nanomedicine*, 6: 863-869.
- 57. Azam, A., Ahmed, F., Habib, S. S., Khan, Z. H., and Salah, N. A. (2013). Fabrication of Co-doped ZnO nanorods for spintronic devices. *Metals and Materials International*, 19: 845-850.
- Medina, M. C., Rojas, D., Flores, P., Peréz-Tijerina, E., and Meléndrez, M. F. (2016). Effect of ZnO nanoparticles obtained by arc discharge on thermomechanical properties of matrix thermoset nanocomposites. *Journal of Applied Polymer Science*, 133(30): 43631.
- Lee, H. J., Yang, U. J., Kim, K. N., Park, S., Kil, K. H., Kim, J. S., ... and Baik, J. M. (2019). Directional Ostwald ripening for producing aligned arrays of nanowires. *Nano Letters*, 19(7): 4306-4313.
- Sridevi, K. P., Sivakumar, S., and Saravanan, K. (2021). Synthesis and characterizations of zinc oxide nanoparticles using various precursors.
 Annals of the Romanian Society for Cell Biology, 2021: 8679-8689.
- 61. Li, H., Wang, J., Liu, H., Zhang, H., and Li, X., (2005). Zinc oxide films prepared by sol–gel method. *Journal of Crystal Growth*, 275(1-2): e943-e946.